

1 **Light pollution alters the skeletal morphology of coral juveniles and impairs their light**  
2 **capture capacity**

3 Netanel Kramer<sup>1,2\*</sup>, Raz Tamir<sup>3</sup>, Claudia Tatiana Galindo-Martínez<sup>4</sup>, Daniel Wangpraseurt<sup>4,5</sup>,  
4 Yossi Loya<sup>1</sup>

5 <sup>1.</sup> *School of Zoology, Tel-Aviv University, Tel Aviv, Israel*

6 <sup>2.</sup> *The Steinhardt Museum of Natural History, Israel National Center for Biodiversity*

7 *Studies, Tel Aviv, Israel*

8 <sup>3.</sup> *Israel Oceanography & Limnological Research, National Institute of Oceanography,*  
9 *Haifa, Israel*

10 <sup>4.</sup> *Marine Biology Research Division, Scripps Institution of Oceanography, University of*  
11 *California San Diego, San Diego, USA*

12 <sup>5.</sup> *Department of Nanoengineering, University of California San Diego, San Diego, USA*

13

14 \* Corresponding author:

15 Netanel Kramer, email: [nati.kramer@gmail.com](mailto:nati.kramer@gmail.com)

16

17

18

19

20

21

22

23

24 **Keywords:** Artificial light at night (ALAN); Coral reefs; Light harvesting; Coral morphology;  
25 Photophysiology; Bio-optics

26     **Abstract**

27           Urbanization and infrastructure development have changed the night-time light regime  
28    of many coastal marine habitats. Consequently, Artificial Light at Night (ALAN) is becoming  
29    a global ecological concern, particularly in nearshore coral reef ecosystems. However, the  
30    effects of ALAN on coral architecture and their optical properties are unexplored. Here, we  
31    conducted a long-term *ex situ* experiment (30 months from settlement) on juvenile *Stylophora*  
32    *pistillata* corals grown under ALAN conditions using light-emitting diodes (LEDs) and  
33    fluorescent lamps, mimicking light-polluted habitats. We found that corals exposed to ALAN  
34    exhibited altered skeletal morphology that subsequently resulted in reduced light capture  
35    capacity, while also gaining better structural and optical modifications to increased light levels  
36    than their ambient-light counterparts. Additionally, light-polluted corals developed a more  
37    porous skeleton compared to the control corals. We suggest that ALAN induces light stress in  
38    corals, resulting in a decrease in the solar energy available for photosynthesis during daytime  
39    illumination.

40

41

42

43

44

45

46

47

48

49

50

51        **1. Introduction**

52        Natural light cycles, including sunlight and moonlight, play a crucial role in regulating  
53        various physiological, biological, and behavioral processes in reef-building corals (Iluz and  
54        Dubinsky, 2015; Kaniewska et al., 2015). The increase in urbanization along coastal areas is  
55        exposing marine environments to excessive anthropogenic light sources (Gaston et al., 2015;  
56        Rosenberg et al., 2019; Tamir et al., 2017). The potential damage caused by these artificial  
57        lights to various ecosystems is commonly termed ‘ecological light pollution’ (Longcore and  
58        Rich, 2004). The negative impact of artificial light at night (ALAN) on coastal and marine  
59        environments has only recently been recognized as a novel environmental stressor (Davies and  
60        Smyth, 2018; Tidau et al., 2021). Research on the effects of widespread ALAN exposure on  
61        marine fauna is limited compared with studies on terrestrial organisms (Davies et al., 2014;  
62        Falcón et al., 2020; Hölker et al., 2010). For tropical reef-building corals, artificial lighting  
63        could constitute a major perturbation to nocturnal light regimes, as it disrupts the natural  
64        photoperiod cycle of light and darkness (Lynn and Quijón, 2022; Marangoni et al., 2022).  
65        Consequently, ALAN affects crucial processes synchronized with the diel light-dark cycle of  
66        corals, including metabolism and photophysiology (Ayalon et al., 2021a, 2019; Rosenberg et  
67        al., 2019; Tamir et al., 2020) as well as gametogenesis and spawning synchronicity (Ayalon et  
68        al., 2021b). Recently, light pollution has been shown to induce photoinhibition and oxidative  
69        stress in symbiotic corals (Levy et al., 2020) and might thus play an important role in  
70        modulating the ecophysiology of corals in urban environments.

71        Solar radiation plays a key role in controlling the physiology and morphology of corals  
72        due to the mutualistic symbiosis between the coral host and their photosynthetic dinoflagellate  
73        algae (family: Symbiodiniaceae) (Roth, 2014). Coral have thus adapted to optimize their light  
74        capture mechanisms to enhance the symbiotic relationship in response to varying light  
75        quantities (i.e., intensity) and qualities (i.e., spectrum) (Hoogenboom et al., 2008; Iluz and

76 Dubinsky, 2015; Kahng et al., 2019). For example, corals are well adapted to the harsh  
77 irradiance conditions experienced in shallow-water coral reefs (Wangpraseurt et al., 2014)  
78 through a range of structural and physiological adaptations, including the modulation of  
79 skeletal architecture and host tissue thickness (Kramer et al., 2022b; Wangpraseurt et al., 2012),  
80 as well as the synthesis of photoprotective animal host proteins that modulate light capture and  
81 photosynthesis (Lyndby et al., 2016; Salih et al., 2000). Typically, corals exposed to high-light  
82 conditions have a greater ability to cope with excess light, whereas corals residing in low-light  
83 environments exhibit highly efficient photosynthetic performance (Einbinder et al., 2016;  
84 Kramer et al., 2022c; Martinez et al., 2020).

85 Similar to corals, plant morphology, growth, and development are influenced by light-  
86 driven factors, including day length, light intensity, and light quality (Cope and Bugbee, 2013;  
87 Lee et al., 2007). For instance, some plant species have shown changes in leaf size and  
88 morphology upon exposure to ALAN (Wang et al., 2015; Zheng and Van Labeke, 2017).  
89 However, although extensive research has demonstrated the effects of light pollution on plant  
90 morphology, the impact of these effects on calcifying organisms, apart from corals, remains  
91 relatively unexplored. Nevertheless, a study conducted by Rocha et al. (2014) demonstrated  
92 how different spectral distributions of light can influence coral skeletal architecture at macro-  
93 and micro-scales. That study has shown that corals grown under different light spectra during  
94 the day (photoperiod of 12-hr light: 12-hr dark), emitting the same photosynthetically active  
95 radiation (PAR), exhibited significant morphological variability (i.e., corallite diameter, septal  
96 length, etc.) in two symbiotic scleractinian coral species. Despite this finding, the full extent of  
97 the effect of nocturnal light pollution on the morphological traits and ecophysiological  
98 responses of corals remains largely unknown.

99 Here, we investigated whether light pollution could lead to changes in coral skeletal  
100 morphology and optical properties, thereby affecting their ability to effectively capture light.

101 We conducted a comparative study of *Stylophora pistillata* coral juveniles that grew under  
102 three light conditions (control and two different artificial light treatments) over a period of 30  
103 months starting from settlement. The altered night-time light regime over the long term led to  
104 significant changes in skeletal morphology, algal physiology, and skeletal reflectance,  
105 indicating a host-level response to light-induced stress. Since photosynthesis is a fundamental  
106 process that enables the growth and survival of reef corals, any decline in this process could  
107 disrupt the entire coral reef ecosystem. We thus discuss the potential undesirable decline in  
108 photosynthetic performance by ALAN exposure in coral reefs.

109

## 110 **2. Materials and Methods**

### 111 2.1 Study species and collection

112 Since the shallow waters are in close proximity to the shore, corals at these depths are  
113 significantly more exposed to artificial illumination than deeper ones. *Stylophora pistillata*  
114 corals are interesting to consider with respect to ALAN, as this species dominates the shallow  
115 waters of the Gulf of Eilat/Aqaba (GoE/A), the Red Sea (29.50°N, 34.92°E), from juveniles to  
116 adults (Kramer et al., 2020, 2019; Loya, 1976). It is worth noting that on a global scale, the  
117 northern coast of the GoE/A has been identified as a heavily light-polluted area, with Eilat's  
118 reef night sky brightness being on average 470% brighter than the natural night sky (Ayalon et  
119 al., 2021b; Tamir et al., 2017), thus making it a fundamental location for studying the effects  
120 of ALAN on coral species.

121 The study by Tamir et al. (2020) provided the *S. pistillata* coral juveniles used in this  
122 study. Briefly, planulae were collected in front of the Interuniversity Institute for Marine  
123 Sciences in Eilat (IUI) at shallow-water depths (< 5 m) to avoid phenotypic variations caused  
124 by different light or flow environments. The planulae have settled in three separate open-circuit  
125 seawater tables (i.e., no water exchanged between them; Fig. 1): a control (ambient conditions

126 at night – moonlight only) and two light pollution treatments with distinct spectra in the visible  
127 light wavelengths, which simulated the most common city lighting methods (LED and  
128 fluorescent lamps; Tamir et al. (2017)). The lamps were turned on and off daily using a  
129 photocell sensor, illuminating the same nighttime irradiance levels as those found in nearshore  
130 artificial lighting systems in Eilat ( $1 \times 10^{-6}$   $\mu\text{mol photons m}^{-2} \text{ s}^{-1}$ ; Tamir et al., 2017). For  
131 further details on the experimental setup (e.g., light parameters and spectrum), please see  
132 Methods S1 and Fig. S1. The coral juveniles that survived post-settlement mortality were  
133 maintained and monitored under controlled conditions at the IUI from June 2017 to December  
134 2019.

135

### 136 2.2 Cell density and chlorophyll-a extraction of microalgae symbionts

137 After two and a half years of growth, ten intact juvenile colonies were randomly  
138 sampled from each treatment to determine cell density and chlorophyll-a content. Their tissue  
139 was removed using an airbrush at high pressure with 0.2 nm filtered seawater. Subsequently,  
140 the skeletons were bleached in a 6% sodium hypochlorite solution for 24 h, thoroughly rinsed  
141 with deionized running water to remove the remaining organic matter, and then left to dry at  
142 room temperature for 24 h. The microalgal fraction was extracted from the host tissue by  
143 homogenization and centrifugation (5,000 rpm for 5 min). Samples were then immediately  
144 frozen at -80°C for later analysis. Cell counts were assessed using a hemocytometer on five  
145 replicate micrographs (scaled to 0.1  $\text{mm}^3$ ), then normalized to the coral surface area to measure  
146 algal density ( $\text{cells/cm}^2$ ). Chlorophyll-a was extracted from the remaining algae using 100%  
147 cold acetone for 15 h at 4°C, quantified using spectrophotometry (Ultrospec 2100 pro,  
148 Amersham Pharmacia Biotech, USA), and calculated following Jeffrey and Humphrey (1975).  
149 Chlorophyll-a was normalized to both the surface area ( $\mu\text{g/cm}^2$ ) and algal cells (pg/cell).

150

151 2.3 Morphological analyses

152 To accurately capture the influence of different light conditions on the diversity of coral  
153 skeletal features, morphometric quantitative information was extracted using high-resolution  
154 computed tomography (Nikon XT H 225ST  $\mu$ CT, Nikon Metrology Inc., USA). The coral  
155 skeletons were scanned with a voxel size of 10-15  $\mu$ m (depending on specimen size), 0.25 mm  
156 stainless steel filter, voltage of 65 kV, amperage of 123  $\mu$ A, and exposure time of 1.15 s. Scans  
157 from each specimen were saved in TIFF image format for 3D volume rendering and  
158 quantitative analysis using Dragonfly software (© 2023 Object Research System (ORS) Inc.).  
159 The volume and surface area of each coral juvenile were determined, and nine skeletal  
160 morphological traits were measured from intact corallites and the coenosteum region: calyx  
161 diameter (CD), theca (corallite height) height (TH), septal length (SL), septal width (SW),  
162 columella height (CH), coenosteal spine length (SPL), coenosteal spine width (SPW), corallite  
163 spacing (CS), and coenosteal spine spacing (SS). These traits were chosen because they were  
164 shown to exhibit significant variations in different light environments, highlighting their  
165 importance in understanding complex skeletal architecture and its implications (Kramer et al.,  
166 2022b; Rocha et al., 2014). In addition, the apparent porosity was assessed as the percentage  
167 ratio of the pore volume to the total volume occupied by the coral skeleton.

168

169 2.4 Coral optical measurements

170 To characterize the skeletal optical properties, we measured the diffuse spectral  
171 reflectance (R) and scalar irradiance  $E_0(\lambda)$  of coral juveniles. The samples were placed in a  
172 black acrylic chamber filled with water and illuminated with homogeneous diffuse light  
173 provided by a semi-sphere coated with barium oxide (BaO) and a LED lamp (CRI-MAX TM  
174 PAR 30, Yuji Lighting). R was measured using a flat-cut fiber-optic reflectance probe  
175 (diameter = 0.23 cm, Ocean Insight) connected to a miniature spectrometer (Flame, Ocean

176 Insight;  $n = 5$  scans per measurement, boxcar width = 2 nm, resolution = 0.2 nm) (Enríquez et  
177 al., 2005; Vásquez-Elizondo et al., 2017). The probe was placed 5 mm away from the skeletal  
178 surface at a 45° angle relative to the surface. Three random surface regions per colony ( $n = 8$   
179 colonies) were chosen for the measurements, and the experimental outcomes were normalized  
180 against a 99% diffuse reflectance standard (Spectralon, Labsphere).

181 Scalar irradiance was measured using a fiber-optic scalar irradiance microprobe with a  
182 spherical tip diameter of 80  $\mu\text{m}$  mounted on a micromanipulator (Pyro-Science GmbH,  
183 Germany) (Kramer et al., 2022c; Wangpraseurt et al., 2012). To avoid bias measurements  
184 resulting from nearby branch junction light scattering and optical variability between corallites  
185 and coenosteum,  $E_0(\lambda)$  spectra were measured in three randomly selected areas on the  
186 coenosteum and three corallites near the coral branch tips.  $E_0(\lambda)$  was measured for five coral  
187 juveniles per treatment. After each measurement, reference measurements of the incident  
188 downwelling irradiance  $E_d(\lambda)$  were taken over a black non-reflective surface. The spectral  
189 irradiance  $E_0(\lambda)$  was then normalized to the incident downwelling irradiance  $E_d(\lambda)$ .

190

## 191 2.6 Statistical analyses

192 Statistical analyses were performed using the R software (R Development Team, 2023).  
193 Since in most cases, the data did not conform to parametric test assumptions, variations  
194 between treatments (fixed effect) for each morphological trait were tested using a mixed-effects  
195 permutational analysis (MEPA; 999 permutations), and models included the coral's colony ID  
196 as a random effect. These analyses were performed using the `{lme4}`(Bates et al., 2015) and  
197 `{predictmeans}`(Luo et al., 2022) packages. When significant differences were found, the  
198 standardized effect sizes and 95% confidence intervals (CI; 5000 bootstrap samplings) of the  
199 treatments were estimated by calculating Hedges'  $g$  ( $Hg$ ) using the package `{dabestr}`(Ho et  
200 al., 2019). CIs that did not overlap with zero were considered significant effects. A principal

201 coordinates analysis (PCoA) based on a Euclidean distance matrix of standardized data was  
202 created using the {vegan} package to visualize the pattern of morphological variation between  
203 depths in a multivariate trait space (hereafter, 'morphospace'). Finally, permutational  
204 multivariate analysis of variance (PERMANOVA; 999 permutations) was performed to  
205 determine the overall effect of depth on morphological patterns.

206

### 207 **3. Results**

#### 208 3.1 Skeletal porosity, symbiont cell density, and chlorophyll-a content

209 The coral skeletal porosity (%) differed significantly among the three treatments,  
210 ranging from 6.18% to 22.61% (MEPA,  $p < 0.001$ ; Fig. 2a). The porosity increased by over  
211 two-thirds for corals grown under the LED treatment ( $16.04 \pm 1.45\%$ ; mean  $\pm$  SE) compared  
212 to the control ( $9.15 \pm 0.53\%$ ) and fluorescent ( $11.54 \pm 0.84\%$ ) groups. Likewise, corals in the  
213 fluorescent treatment exhibited a smaller but significant porosity increase compared with the  
214 control group ( $Hg = 1.19$  [CI<sub>95%</sub> 0.162; 2.25]). Juvenile corals grown under fluorescent light  
215 exhibited the highest areal chlorophyll-a content ( $\mu\text{g chl cm}^{-2}$ ; Fig. 2b), whereas no significant  
216 difference was observed between the control and LED treatment groups ( $Hg = 0.169$  [CI<sub>95%</sub> -  
217 0.731; 1.16]). Similarly, algal symbiont density ( $\text{cells cm}^{-2}$ ; Fig. 2c) was the highest in the  
218 fluorescent group, however, a marked four-fold reduction was observed in LED-grown corals  
219 compared to the fluorescent group ( $Hg = -3.90$  [CI<sub>95%</sub> -5.22; -2.75]), exhibiting the lowest  
220 concentration levels among treatments ( $1.81 \times 10^5$   $\text{cells cm}^{-2}$ ). The cellular chlorophyll-a  
221 content ( $\text{pg cell}^{-1}$ ; Fig. 2d) was significantly influenced by LED lighting, with a three-fold  
222 increase (MEPA,  $p < 0.001$ ), while the control and fluorescent treatments showed similar  
223 concentrations ( $Hg = 0.33$  [CI<sub>95%</sub> -0.52; 1.24]).

224

#### 225 3.2 Morphometrics

226                   Thirty months post-settlement, juvenile *S. pistillata* colonies exhibited three distinct  
227                   morphotypes among the three illumination methods (PERMANOVA,  $p < 0.001$ ; Figs. 3, 4).  
228                   The first two PCOA axes explained 66.89% of the total variation in the morphospace among  
229                   the light treatments (Fig. 4). The first axis explained 45.32% of the variance with over half of  
230                   the contribution deriving from calyx diameter (CD), theca height (TH), and septal length (SL).  
231                   Substantial differences were observed in all traits among the three treatments, except for  
232                   corallite spacing (CS) which was statistically non-significant (MEPA,  $p = 0.469$ , Fig. 3f).  
233                   Generally, both or one of the ALAN conditions led to larger morphological trait sizes compared  
234                   to their control counterparts. For example, the calyx diameter (CD) was 9% wider in LED-  
235                   grown corals than in corals grown under moonlight and fluorescent light (MEPA,  $p < 0.001$ ;  
236                   Fig. 3b). In certain instances, both LED and fluorescent treatments exhibited similar trends; for  
237                   example, the light-polluted conditions led to corallites that were substantially deeper (i.e., 21%  
238                   increase in theca height (TH)) than their control counterparts (MEPA,  $p < 0.001$ ; Fig 3c).

239

240                   3.3 Skeletal optical properties

241                   The light field parameters ( $R$  and  $E_0$ ) were significantly different among the treatments.  
242                   The coral specimens subjected to light pollution displayed significantly diminished skeletal  
243                   reflectance ( $R$ ) compared to the control group ( $70.20 \pm 0.44\%$ ; mean  $\pm$  SE; at  $\lambda = 675$  nm),  
244                   with percentages of  $61.30 \pm 0.44\%$  and  $66.80 \pm 0.8\%$  for LED and fluorescent-treated corals,  
245                   respectively (Fig. 5a; MEPA,  $p < 0.01$ ). Similarly, LED had a stronger effect on the percentage  
246                   of the incident downwelling irradiance ( $E_0$ ; at  $\lambda = 675$  nm) measured at the corallite surface,  
247                   exhibiting nearly 50% lower  $E_0$  than the control counterparts (Fig. 5b;  $201.86 \pm 2.08\%$  vs.  
248                    $247.06 \pm 2.05\%$ ;  $Hg = -2.33$  [CI95% -2.68; -1.96]), whereas the fluorescent-grown corals  
249                   exhibited a smaller yet significant reduction in the spectral irradiance ( $238.06 \pm 2.55\%$ ;  $Hg = -$   
250                    $0.41$  [CI95% -0.71; -0.12]). Likewise,  $E_0$  measurements over the coenosteum revealed lower

251 values for the light-polluted corals (MEPA,  $p < 0.01$ ; Fig. 5c), exhibiting a 46% and 11% E<sub>0</sub>  
252 reduction in the LED and fluorescent treatments, respectively.

253

254 **4. Discussion**

255 Light plays a critical role in the development and survival of scleractinian corals, as it  
256 provides energy through photosymbiotic algae residing within the coral's tissue (Roth, 2014).  
257 Therefore, maintaining a delicate balance between light quality and quantity is essential for  
258 corals to thrive and sustain healthy coral reef ecosystems. Yet, our understanding of light  
259 pollution and its impact on marine environments is still in its early stages. Since corals at the  
260 northern GoE/A are increasingly and constantly confronted with exposure to ALAN, it is  
261 expected that ALAN plays a significant role in shaping the essential aspects of coral light  
262 harvesting. One of the key aspects is the complex skeletal architecture of corals, which creates  
263 a variety of light microhabitats (Enríquez et al., 2017). As a result, corals are expected to exhibit  
264 a morphological structure that adequately supports the amount of light reaching their  
265 photosymbionts.

266 Here, we show that long-term exposure to ALAN induces noticeable physiological,  
267 optical, and morphological changes in *S. pistillata* juveniles, revealing three distinct  
268 morphotypes (Figs. 1b, 4). We suggest that exposure to ALAN may have complex effects on  
269 symbiont physiology and coral skeletal growth and structure. Owing to the higher photon  
270 energy (i.e., receiving more photons from higher wavelength frequencies) than that of the  
271 ambient-light corals, the experimental corals exposed to artificial nocturnal light exhibited  
272 lower light capture demands for photosynthesis.

273

274 4.1 Morphometrics and optical properties

275 The skeletal morphology of light-polluted corals appears to resemble that of corals  
276 inhabiting “high-light” environments in comparison with the control group (Einbinder et al.,  
277 2016; Kramer et al., 2022b, 2022c; Malik et al., 2020; Tamir et al., 2020). Coral juveniles under  
278 ALAN exhibited skeletal characteristics and optical properties that make them better suited to  
279 handle higher levels of photon flux, presumably because of the additional light acquired at  
280 night.

281 We found that among the morphological traits, theca height (TH), calyx diameter  
282 (SPL), and septal length (SL; the vertical structures that divide the corallites) were the most  
283 influential traits that were affected by varying light spectra at night. Several previous studies  
284 have established that these skeletal characteristics play a key role in determining the amount of  
285 light that can reach the photosymbionts (Kramer et al., 2022b; Ow and Todd, 2010; Studivan  
286 et al., 2019; Swain et al., 2018). While all skeletal traits have a certain degree of influence on  
287 the coral's light environment, these traits are considered particularly relevant in shaping the  
288 surface complexity. We showed that the morphological traits of corals exposed to either one or  
289 both ALAN conditions generally exhibited larger trait sizes than those grown under the natural  
290 night sky regime (Fig. 3). Deeper and larger corallites, taller columella, longer septa, and longer  
291 coenosteal spines, for example, contribute to the complexity of the skeletal architecture and  
292 can affect the direction and intensity of light reaching the microalgae, thereby altering their  
293 light exposure (Kramer et al., 2022b). They create a more convoluted surface that allows for  
294 better self-shading in increased light environments, thus preventing photodamage to the  
295 photosymbionts due to excess light.

296 Additionally, optical measurements performed on the skeletons of corals exposed to  
297 light pollution revealed a significant reduction in both bulk light reflection and spectral  
298 irradiance near the skeletal surface compared to the control group (Fig. 5). In particular, LED  
299 had a more significant impact on the coral juveniles light field than the fluorescent lighting.

300 The data suggests a photo-acclimation to the altered light regime by reducing excess *in hospite*  
301 light exposure of Symbiodiniaceae. This phenomenon has also been observed in a study  
302 comparing shallow and mesophotic optical properties, revealing a reduced skeletal  
303 backscattered light under high-light levels (Kramer et al., 2022c). Other factors that regulate  
304 the availability of photons for photosynthesis, such as the spatial distribution of the symbiotic  
305 algae in the tissue layer or the presence of coral fluorescent pigments (FPs) (Lyndby et al.,  
306 2016), could also potentially be influenced by ALAN and consequently impact the coral's  
307 internal light environment. However, investigating these aspects was beyond the scope of this  
308 study, highlighting the need for further research in these areas.

309 Given these results, our findings support the notion that light-driven changes often  
310 occur in parallel between the host's morphology, algal physiology, and optical properties  
311 (Enríquez et al., 2017; Kramer et al., 2022c; Swain et al., 2018). We show that the optical traits  
312 of the coral host skeleton complement the photosynthetic demands of coral photosymbionts,  
313 that is, the lower algal cell densities are compensated by the reduced light available from the  
314 skeleton, thereby preventing photodamage. Since photosynthesis and energy production in  
315 corals are primarily carried out by the photosymbionts, the observed skeletal changes may also  
316 be linked to the altered symbiont physiology caused by ALAN (Fig. 2), as previous research  
317 has highlighted the crucial role of symbiotic algae in coral calcification and skeletal growth  
318 (Goreau, 1959; Mass et al., 2007). Moreover, we can infer that the observed changes imply a  
319 level of light-induced stress under altered nightlight conditions, as both the symbiont and the  
320 host's traits appear to have reduced the potential for the oversaturation (i.e., photoinhibition)  
321 of the photosystem complexes.

322

323 4.2 Porosity

324 The  $\mu$ CT analysis revealed that light-polluted corals were substantially more porous  
325 than their control counterparts (Fig. 2a). While Rocha et al. (2014) previously reported no  
326 significant changes in the skeletal porosity of *S. pistillata* that were only exposed to different  
327 daytime spectra, our results indicate that changes in the internal void space of coral skeletons  
328 depend not only on the combination of sunlight intensity and spectrum (Kramer et al., 2022b;  
329 Malik et al., 2020), but also on the night-time light spectrum. Interestingly, despite showing  
330 the fastest growth rate among the three treatments (Tamir et al., 2020), coral juveniles grown  
331 under the LED light exhibited similar porosity values to their slow-growing conspecifics found  
332 in low-light depths (Kramer et al., 2022b). This suggests that the growth rate of a given coral  
333 species may not be the sole determinant of its skeletal porosity, and implies that other factors  
334 such as water chemistry, temperature, and light, may play a crucial role in determining the  
335 porosity of coral skeletons (Fantazzini et al., 2015; Foster et al., 2016; Kramer et al., 2022b).

336

### 337 4.3 Insights on the effect of ALAN on coral growth

338 Only a limited number of studies have evaluated the effects of ALAN on the growth of  
339 marine organisms (Marangoni et al., 2022), let alone in reef-building corals. This study  
340 demonstrates that the spectral composition of the artificial light sources used for night-time  
341 illumination, which differs from that of night sky illumination (Tamir et al., 2017), may have  
342 a substantial adverse impact on coral skeletal growth, structure, and physical properties.

343 As expected, light-polluted corals exhibited either decreased symbiont cell density or  
344 reduced cellular chlorophyll-*a* (Fig. 2; Ayalon et al., 2019; Levy et al., 2020; Rosenberg et al.,  
345 2019). Specifically, LED-grown juvenile corals exhibited a paler surface color resembling  
346 lightly bleached corals, which was consistent with their reduced photosynthetic activity, as  
347 shown by Tamir et al. (2020). However, surprisingly, that study has also shown that despite  
348 lower photosynthetic rates during the day and negligible photosynthesis at night (light intensity

349 = 0.8  $\mu\text{mol photons m}^{-2} \text{s}^{-1}$ , which is significantly lower than the photosynthetic compensation  
350 point), corals illuminated by LED lighting exhibited enhanced calcification rates at night and  
351 produced greater colony structures, as shown in Fig. 1b. This may be explained by the higher  
352 blue peak (i.e., greater photon energy) and broader spectrum prevalent under LED lighting,  
353 inducing light-enhanced calcification (LEC). As seawater in the open ocean attenuates blue  
354 light the least, many marine organisms are sensitive to this spectral region (Marshall et al.,  
355 2015). Specifically, corals possess an array of sensitive photoreceptors that mainly absorb in  
356 the blue region of the light spectrum (Gorbunov and Falkowski, 2002; Levy et al., 2007). As  
357 demonstrated by previous studies, blue light can enhance calcification rates in hermatypic  
358 corals despite reduced photosynthesis, suggesting that the effect of light on LEC is not solely  
359 due to photosynthetic energy, but may involve direct signaling through the host's receptors  
360 (Cohen et al., 2016; Eyal et al., 2019). Therefore, cumulative exposure to sunlight and LED at  
361 night may increase total energy production and ultimately promote coral growth. As such, our  
362 results provide evidence of increased skeletal growth despite the lower photosynthetic activity,  
363 supporting the assumption that blue-light absorbing photoreceptors activate other physiological  
364 processes (e.g., proton  $[\text{H}^+]$  pumps,  $\text{Ca}^{2+}$ -ATPase pumps, etc.) to further induce coral  
365 calcification at night.

366 A study on the effects of exposure to ALAN on coral reef fish larvae during the  
367 recruitment stage found that while ALAN-exposed fish grew faster, they also experienced  
368 changes in behavior, higher susceptibility to predation, and significantly higher mortality rates  
369 (O'Connor et al., 2019). Similarly, as previous studies proposed, faster coral growth rates are  
370 not a reliable indicator for coral health since it does not necessarily confer advantages or  
371 optimize the fitness of corals, but rather there is a trade-off between energy allocation for coral  
372 growth and fecundity (Darling et al., 2012; Edinger et al., 2000; Harrison and Wallace, 1990;  
373 Kramer et al., 2022a; Loya et al., 2004). For example, Loya et al. (2004) found that although

374 coral growth is accelerated under chronic eutrophication, it also renders corals more susceptible  
375 to lower reproductive output. As previously mentioned, corals exposed to photopollution at  
376 night exhibit lower fecundity (Ayalon et al., 2021b), which subsequently reduces the supply of  
377 planulae and further hinders successful settlement (Tamir et al., 2020). Taken together with  
378 previous research, we suggest that ALAN may favor faster coral growth at the cost of reduced  
379 reproductive investment (Ayalon et al., 2021b; Loya et al., 2004; Tamir et al., 2020).

380

381 4.4 Additional potential detrimental effects of light pollution in corals

382 In addition to light pollution, coral reef ecosystems are already subjected to  
383 unprecedented degradation, resulting mainly from warming oceans (Leggat et al., 2019) as well  
384 as a growing threat from the uptake of anthropogenic carbon dioxide (Jiang et al., 2019). Coral  
385 juveniles subjected to elevated temperatures and ocean acidification, for example, have been  
386 shown to impair their skeletal structures (Foster et al., 2016). Thus, the interaction of these  
387 stressors with light pollution may further weaken skeletal structures, making them more  
388 vulnerable to damage from physical disturbances, predation, or harmful boring organisms.

389 We further suggest that light pollution may render corals more susceptible to thermal  
390 stress. For example, in the already symbiont-depleted tissue of LED-grown corals, one factor  
391 that can contribute to this process is the enhanced light flux promoted by the reflection of the  
392 incident light from the coral skeleton, which can further stimulate the loss of endosymbiotic  
393 algae and exacerbate the bleaching process, leading to an optical feedback loop (Wangpraseurt  
394 et al., 2017).

395 It is important to note that because of its higher energy efficiency and longer lifespan,  
396 many coastal regions have transitioned towards LED lighting to replace older lighting systems.  
397 LED lighting is anticipated to contribute 97% of the global lighting market by 2025 (Smyth et  
398 al., 2021; Zissis and Bertoldi, 2018). However, although our results show that LED lighting

399 has more pronounced effects on coral skeletal characteristics and photosymbiont physiology,  
400 the significance of fluorescent lighting should not be deemed less important. In areas where  
401 fluorescent lighting is still in use along urbanized near-shore coral reefs, it can still have  
402 moderate negative effects on coral biology. Given the expected increase in ocean warming and  
403 the global transition towards LED lighting in coastal urban regions in the coming decades,  
404 future research should explore the potential synergetic effects of ALAN and global climate  
405 change stressors.

406

## 407 **5. Conclusions**

408 We demonstrated that ongoing exposure to nocturnal artificial illumination can alter the  
409 skeletal architecture and optical properties of shallow-water juvenile corals, which in turn  
410 affects their light microenvironment. However, it is important to note that the effects of ALAN  
411 on photosymbiotic corals are complex and depend on various factors, such as the intensity,  
412 spectrum, and duration of night-light exposure, as well as on the respective coral species and  
413 their developmental stage. Thus, to gain a comprehensive understanding of the detrimental  
414 impacts of light pollution from coastal cities on benthic ecosystems, we advocate for  
415 conducting long-term studies to investigate the impacts of ALAN exposure from juveniles to  
416 adulthood. Given the significant role of light in various marine coastal fauna, preserving the  
417 natural underwater light regime should be a priority for coral reef conservation, making it an  
418 essential factor to consider in local coral reef management.

419

## 420 **Acknowledgments**

421 We are grateful to the Interuniversity Institute for Marine Sciences in Eilat (IUI) for  
422 making its facilities available. We thank S. Ellenbogen from the Dan David Center for Human  
423 Evolution and Biohistory Research for her technical assistance with the  $\mu$ CT. This work was

424 supported by the joint United States National Science Foundation (NSF) and United States –  
425 Israel Binational Science Foundation (NSF-BSF) grant No. 2021647 to Y.L., and No. 2149925  
426 to D.W. and Martin Tresguerres, and by the PADI Foundation No. 74641 to N.K.

427

428 **Author contributions**

429 N.K. and Y.L. conceived and designed the study; N.K., R.T., and C.T.G.M. executed  
430 the experiment; N.K. performed data analyses and generated figures; Y.L. and D.W. supervised  
431 the study; N.K. wrote the original manuscript with contributions and final approval from all  
432 authors.

433

434 **Competing interests**

435 The authors declare no competing interests.

436

437 **References**

438 Ayalon, I., Benichou, J.I.C., Avisar, D., Levy, O., 2021a. The Endosymbiotic Coral Algae  
439 Symbiodiniaceae Are Sensitive to a Sensory Pollutant: Artificial Light at Night, ALAN.  
440 *Front Physiol* 12, 897. <https://doi.org/10.3389/fphys.2021.695083>

441 Ayalon, I., de Barros Marangoni, L.F., Benichou, J.I.C., Avisar, D., Levy, O., 2019. Red Sea  
442 corals under Artificial Light Pollution at Night (ALAN) undergo oxidative stress and  
443 photosynthetic impairment. *Glob Chang Biol* 25, 4194–4207.  
444 <https://doi.org/10.1111/gcb.14795>

445 Ayalon, I., Rosenberg, Y., Benichou, J.I.C., Campos, C.L.D., Sayco, S.L.G., Nada, M.A.L.,  
446 Baquiran, J.I.P., Ligson, C.A., Avisar, D., Conaco, C., Kuechly, H.U., Kyba, C.C.M.,  
447 Cabaitan, P.C., Levy, O., 2021b. Coral Gametogenesis Collapse under Artificial Light  
448 Pollution. *Current Biology* 31, 413-419.e3.  
449 <https://doi.org/https://doi.org/10.1016/j.cub.2020.10.039>

450 Bates, D., Mächler, M., Bolker, B., Walker, S., 2015. Fitting Linear Mixed-Effects Models  
451 Using `{lme4}`. *J Stat Softw* 67, 1–48. <https://doi.org/10.18637/jss.v067.i01>

452 Cohen, I., Dubinsky, Z., Erez, J., 2016. Light Enhanced Calcification in Hermatypic Corals:  
453 New Insights from Light Spectral Responses. *Front Mar Sci* 2.  
454 <https://doi.org/10.3389/fmars.2015.00122>

455 Cope, K.R., Bugbee, B., 2013. Spectral Effects of Three Types of White Light-emitting  
456 Diodes on Plant Growth and Development: Absolute versus Relative Amounts of Blue  
457 Light. *Hortscience* 48, 504–509.

458 Darling, E.S., Alvarez-Filip, L., Oliver, T.A., McClanahan, T.R., Côté, I.M., 2012.  
459 Evaluating life-history strategies of reef corals from species traits. *Ecol Lett* 15, 1378–  
460 1386. <https://doi.org/10.1111/j.1461-0248.2012.01861.x>

461 Davies, T.W., Duffy, J.P., Bennie, J., Gaston, K.J., 2014. The nature, extent, and ecological  
462 implications of marine light pollution. *Front Ecol Environ* 12, 347–355.  
463 <https://doi.org/10.1890/130281>

464 Davies, T.W., Smyth, T., 2018. Why artificial light at night should be a focus for global  
465 change research in the 21st century. *Glob Chang Biol* 24, 872–882.  
466 <https://doi.org/https://doi.org/10.1111/gcb.13927>

467 Edinger, E.N., Limmon, G. V., Jompa, J., Widjatmoko, W., Heikoop, J.M., Risk, M.J., 2000.  
468 Normal coral growth rates on dying reefs: Are coral growth rates good indicators of reef  
469 health? *Mar Pollut Bull* 40, 404–425. [https://doi.org/10.1016/S0025-326X\(99\)00237-4](https://doi.org/10.1016/S0025-326X(99)00237-4)

470 Einbinder, S., Gruber, D.F., Salomon, E., Liran, O., Keren, N., Tchernov, D., 2016. Novel  
471 Adaptive Photosynthetic Characteristics of Mesophotic Symbiotic Microalgae within the  
472 Reef-Building Coral, *Stylophora pistillata*. *Front Mar Sci* 3, 195.  
473 <https://doi.org/10.3389/fmars.2016.00195>

474 Enríquez, S., Méndez, E.R., Hoegh-Guldberg, O., Iglesias-Prieto, R., 2017. Key functional  
475 role of the optical properties of coral skeletons in coral ecology and evolution.  
476 *Proceedings of the Royal Society B: Biological Sciences* 284.  
477 <https://doi.org/10.1098/rspb.2016.1667>

478 Enríquez, S., Méndez, E.R., Iglesias-Prieto, R., 2005. Multiple scattering on coral skeletons  
479 enhances light absorption by symbiotic algae. *Limnol Oceanogr* 50, 1025–1032.  
480 <https://doi.org/10.4319/lo.2005.50.4.1025>

481 Eyal, G., Cohen, I., Eyal-Shaham, L., Ben-Zvi, O., Tikochinsky, Y., Loya, Y., 2019.  
482 Photoacclimation and induction of light-enhanced calcification in the mesophotic coral  
483 *Euphyllia paradoxa*. *R Soc Open Sci* 6, 180527. <https://doi.org/10.1098/rsos.180527>

484 Falcón, J., Torriglia, A., Attia, D., Viénot, F., Gronfier, C., Behar-Cohen, F., Martinsons, C.,  
485 Hicks, D., 2020. Exposure to Artificial Light at Night and the Consequences for Flora,  
486 Fauna, and Ecosystems. *Front Neurosci* 14, 1183.  
487 <https://doi.org/10.3389/fnins.2020.602796>

488 Fantazzini, P., Mengoli, S., Pasquini, L., Bortolotti, V., Brizi, L., Mariani, M., di Giosia, M.,  
489 Fermani, S., Capaccioni, B., Caroselli, E., Prada, F., Zaccanti, F., Levy, O., Dubinsky,  
490 Z., Kaandorp, J.A., Konglerd, P., Hammel, J.U., Dauphin, Y., Cuif, J.P., Weaver, J.C.,  
491 Fabricius, K.E., Wagermaier, W., Fratzl, P., Falini, G., Goffredo, S., 2015. Gains and  
492 losses of coral skeletal porosity changes with ocean acidification acclimation. *Nat  
493 Commun* 6. <https://doi.org/10.1038/ncomms8785>

494 Foster, T., Falter, J.L., McCulloch, M.T., Clode, P.L., 2016. Ocean acidification causes  
495 structural deformities in juvenile coral skeletons. *Sci Adv* 2, 1–8.  
496 <https://doi.org/10.1126/sciadv.1501130>

497 Gaston, K.J., Visser, M.E., Hölker, F., 2015. The biological impacts of artificial light at night:  
498 The research challenge. *Philosophical Transactions of the Royal Society B: Biological  
499 Sciences* 370. <https://doi.org/10.1098/rstb.2014.0133>

500 Gorbunov, M.Y., Falkowski, P.G., 2002. Photoreceptors in the cnidarian hosts allow  
501 symbiotic corals to sense blue moonlight. *Limnol Oceanogr* 47, 309–315.  
502 <https://doi.org/https://doi.org/10.4319/lo.2002.47.1.0309>

503 Goreau, T., 1959. The Physiology of Skeleton Formation in Corals. I. A Method for  
504 Measuring the Rate of Calcium Deposition by Corals under Different Conditions.  
505 *Biological Bulletin* 116. <https://doi.org/10.2307/1539156>

506 Harrison, P.L., Wallace, C.C., 1990. Reproduction, dispersal and recruitment of scleractinian  
507 corals, in: Dubinsky, Z. (Ed.), *Ecosystems of the World*. Elsevier, Amsterdam, pp. 133–  
508 206.

509 Ho, J., Tumkaya, T., Aryal, S., Choi, H., Claridge-Chang, A., 2019. Moving beyond P values:  
510 data analysis with estimation graphics. *Nat Methods* 16, 565–566.  
511 <https://doi.org/10.1038/s41592-019-0470-3>

512 Hölker, F., Wolter, C., Perkin, E.K., Tockner, K., 2010. Light pollution as a biodiversity  
513 threat. *Trends Ecol Evol* 25, 681–682.  
514 <https://doi.org/https://doi.org/10.1016/j.tree.2010.09.007>

515 Hoogenboom, M.O., Connolly, S.R., Anthony, K.R.N., 2008. Interactions between  
516 morphological and physiological plasticity optimize energy acquisition in corals.  
517 *Ecology* 89, 1144–1154. <https://doi.org/https://doi.org/10.1890/07-1272.1>

518 Iluz, D., Dubinsky, Z., 2015. Coral photobiology: New light on old views. *Zoology* 118, 71–  
519 78. <https://doi.org/10.1016/j.zool.2014.08.003>

520 Jeffrey, S.W., Humphrey, G.F., 1975. New spectrophotometric equations for determining  
521 chlorophylls a, b, c1 and c2 in higher plants, algae and natural phytoplankton.  
522 *Biochemie und Physiologie der Pflanzen*. [https://doi.org/10.1016/s0015-3796\(17\)30778-3](https://doi.org/10.1016/s0015-3796(17)30778-3)

524 Jiang, L.-Q., Carter, B.R., Feely, R.A., Lauvset, S.K., Olsen, A., 2019. Surface ocean pH and  
525 buffer capacity: past, present and future. *Sci Rep* 9, 18624.  
526 <https://doi.org/10.1038/s41598-019-55039-4>

527 Kahng, S.E., Akkaynak, D., Shlesinger, T., Hochberg, E.J., Wiedenmann, J., Tamir, R.,  
528 Tchernov, D., 2019. Light, Temperature, Photosynthesis, Heterotrophy, and the Lower  
529 Depth Limits of Mesophotic Coral Ecosystems, in: Loya, Y., Puglise, K.A., Bridge,  
530 T.C.L. (Eds.), *Mesophotic Coral Ecosystems*. Springer International Publishing, Cham,  
531 pp. 801–828. [https://doi.org/10.1007/978-3-319-92735-0\\_42](https://doi.org/10.1007/978-3-319-92735-0_42)

532 Kaniewska, P., Alon, S., Karako-Lampert, S., Hoegh-Guldberg, O., Levy, O., 2015.  
533 Signaling cascades and the importance of moonlight in coral broadcast mass spawning.  
534 *eLife* 4, e09991. <https://doi.org/10.7554/eLife.09991>

535 Kramer, N., Eyal, G., Tamir, R., Loya, Y., 2022a. Growth and survival dynamics of  
536 mesophotic coral juveniles in shallow reefs. *Mar Ecol Prog Ser* 682, 237–242.  
537 <https://doi.org/https://doi.org/10.3354/meps13956>

538 Kramer, N., Eyal, G., Tamir, R., Loya, Y., 2019. Upper mesophotic depths in the coral reefs  
539 of Eilat, Red Sea, offer suitable refuge grounds for coral settlement. *Sci Rep* 9, 2263.  
540 <https://doi.org/10.1038/s41598-019-38795-1>

541 Kramer, N., Guan, J., Chen, S., Wangpraseurt, D., Loya, Y., 2022b. Morpho-functional traits  
542 of the coral *Stylophora pistillata* enhance light capture for photosynthesis at mesophotic  
543 depths. *Commun Biol* 5, 861. <https://doi.org/10.1038/s42003-022-03829-4>

544 Kramer, N., Tamir, R., Ben-Zvi, O., Jacques, S.L., Loya, Y., Wangpraseurt, D., 2022c.  
545 Efficient light-harvesting of mesophotic corals is facilitated by coral optical traits. *Funct  
546 Ecol* 36, 406–418. <https://doi.org/10.1111/1365-2435.13948>

547 Kramer, N., Tamir, R., Eyal, G., Loya, Y., 2020. Coral Morphology Portrays the Spatial  
548 Distribution and Population Size-Structure Along a 5–100 m Depth Gradient. *Front Mar  
549 Sci* 7, 615. <https://doi.org/10.3389/fmars.2020.00615>

550 Lee, S.-H., Tewari, R.K., Hahn, E., Paek, K., 2007. Photon flux density and light quality  
551 induce changes in growth, stomatal development, photosynthesis and transpiration of  
552 *Withania Somnifera* (L.) Dunal. plantlets. *Plant Cell Tissue Organ Cult* 90, 141–151.

553 Leggat, W.P., Camp, E.F., Suggett, D.J., Heron, S.F., Fordyce, A.J., Gardner, S., Deakin, L.,  
554 Turner, M., Beeching, L.J., Kuzhiumparambil, U., Eakin, C.M., Ainsworth, T.D., 2019.  
555 Rapid Coral Decay Is Associated with Marine Heatwave Mortality Events on Reefs.  
556 *Current Biology* 1–8. <https://doi.org/10.1016/j.cub.2019.06.077>

557 Levy, O., Appelbaum, L., Leggat, W., Gothlif, Y., Hayward, D.C., Miller, D.J., Hoegh-  
558 Guldberg, O., 2007. Light-Responsive Cryptochromes from a Simple Multicellular  
559 Animal, the Coral *Acropora millepora*. *Science* (1979) 318, 467–470.  
560 <https://doi.org/10.1126/science.1145432>

561 Levy, O., Fernandes de Barros Marangoni, L., I. C. Benichou, J., Rottier, C., Béraud, E.,  
562 Grover, R., Ferrier-Pagès, C., 2020. Artificial light at night (ALAN) alters the  
563 physiology and biochemistry of symbiotic reef building corals. *Environmental Pollution*  
564 266, 114987. <https://doi.org/https://doi.org/10.1016/j.envpol.2020.114987>

565 Longcore, T., Rich, C., 2004. Ecological light pollution. *Front Ecol Environ* 2, 191–198.  
566 [https://doi.org/https://doi.org/10.1890/1540-9295\(2004\)002\[0191:ELP\]2.0.CO;2](https://doi.org/https://doi.org/10.1890/1540-9295(2004)002[0191:ELP]2.0.CO;2)

567 Loya, Y., 1976. The Red Sea coral *Stylophora pistillata* is an r strategist. *Nature* 259, 478–  
568 480. <https://doi.org/10.1038/260170a0>

569 Loya, Y., Lubinevsky, H., Rosenfeld, M., Kramarsky-Winter, E., 2004. Nutrient enrichment  
570 caused by in situ fish farms at Eilat, Red Sea is detrimental to coral reproduction. *Mar  
571 Pollut Bull* 49, 344–353. <https://doi.org/10.1016/j.marpolbul.2004.06.011>

572 Luo, D., Ganesh, S., Koolaard, J., 2022. predictmeans: Calculate Predicted Means for Linear  
573 Models. <https://doi.org/http://cran.r-project.org/package=predictmeans>

574 Lyndby, N.H., Kühl, M., Wangpraseurt, D., 2016. Heat generation and light scattering of  
575 green fluorescent protein-like pigments in coral tissue. *Sci Rep* 6, 26599.  
576 <https://doi.org/10.1038/srep26599>

577 Lynn, K.D., Quijón, P.A., 2022. Casting a light on the shoreline: The influence of light  
578 pollution on intertidal settings. *Front Ecol Evol* 10.  
579 <https://doi.org/10.3389/fevo.2022.980776>

580 Malik, A., Einbinder, S., Martinez, S., Tchernov, D., Haviv, S., Almuly, R., Zaslansky, P.,  
581 Polishchuk, I., Pokroy, B., Stolarski, J., Mass, T., 2020. Molecular and skeletal  
582 fingerprints of scleractinian coral biomineralization: From the sea surface to mesophotic  
583 depths. *Acta Biomater* 1–14. <https://doi.org/10.1016/j.actbio.2020.01.010>

584 Marangoni, L.F.B., Davies, T., Smyth, T., Rodríguez, A., Hamann, M., Duarte, C., Pendoley,  
585 K., Berge, J., Maggi, E., Levy, O., 2022. Impacts of artificial light at night in marine  
586 ecosystems—A review. *Glob Chang Biol* n/a.  
587 <https://doi.org/https://doi.org/10.1111/gcb.16264>

588 Marshall, J., Carleton, K.L., Cronin, T., 2015. Colour vision in marine organisms. *Curr Opin  
589 Neurobiol* 34, 86–94. <https://doi.org/https://doi.org/10.1016/j.conb.2015.02.002>

590 Martinez, S., Kolodny, Y., Shemesh, E., Scucchia, F., Nevo, R., Levin-Zaidman, S., Paltiel,  
591 Y., Keren, N., Tchernov, D., Mass, T., 2020. Energy Sources of the Depth-Generalist  
592 Mixotrophic Coral *Stylophora pistillata*. *Front Mar Sci* 7, 1–16.  
593 <https://doi.org/10.3389/fmars.2020.566663>

594 Mass, T., Einbinder, S., Brokovich, E., Shashar, N., Vago, R., Erez, J., Dubinsky, Z., 2007.  
595 Photoacclimation of *Stylophora pistillata* to light extremes: Metabolism and  
596 calcification. *Mar Ecol Prog Ser* 334, 93–102. <https://doi.org/10.3354/meps334093>

597 O'Connor, J.J., Fobert, E.K., Besson, M., Jacob, H., Lecchini, D., 2019. Live fast, die young:  
598 Behavioural and physiological impacts of light pollution on a marine fish during larval  
599 recruitment. *Mar Pollut Bull* 146, 908–914.  
600 <https://doi.org/https://doi.org/10.1016/j.marpolbul.2019.05.038>

601 Ow, Y.X., Todd, P.A., 2010. Light-induced morphological plasticity in the scleractinian coral  
602 *Goniastrea pectinata* and its functional significance. *Coral Reefs* 29, 797–808.  
603 <https://doi.org/10.1007/s00338-010-0631-4>

604 Rocha, R.J.M., Silva, A.M.B., Vaz Fernandes, M.H., Cruz, I.C.S., Rosa, R., Calado, R., 2014.  
605 Contrasting light spectra constrain the macro and microstructures of scleractinian corals.  
606 *PLoS One* 9, e105863. <https://doi.org/10.1371/journal.pone.0105863>

607 Rosenberg, Y., Doniger, T., Levy, O., 2019. Sustainability of coral reefs are affected by  
608 ecological light pollution in the Gulf of Aqaba/Eilat. *Commun Biol* 2, 289.  
609 <https://doi.org/10.1038/s42003-019-0548-6>

610 Roth, M.S., 2014. The engine of the reef: Photobiology of the coral-algal symbiosis. *Front  
611 Microbiol* 5, 1–22. <https://doi.org/10.3389/fmicb.2014.00422>

612 Salih, A., Larkum, A., Cox, G., Kühl, M., Hoegh-Guldberg, O., 2000. Fluorescent pigments  
613 in corals are photoprotective. *Nature* 408, 850–853. <https://doi.org/10.1038/35048564>

614 Smyth, T.J., Wright, A.E., McKee, D., Tidau, S., Tamir, R., Dubinsky, Z., Iluz, D., Davies,  
615 T.W., 2021. A global atlas of artificial light at night under the sea. *Elementa: Science of*  
616 *the Anthropocene* 9, 49. <https://doi.org/10.1525/elementa.2021.00049>

617 Studivan, M.S., Milstein, G., Voss, J.D., 2019. *Montastraea cavernosa* corallite structure  
618 demonstrates distinct morphotypes across shallow and mesophotic depth zones in the  
619 Gulf of Mexico. *PLoS One* 14. <https://doi.org/10.1371/journal.pone.0203732>

620 Swain, T.D., Lax, S., Lake, N., Grooms, H., Backman, V., Marcelino, L.A., 2018. Relating  
621 Coral Skeletal Structures at Different Length Scales to Growth, Light Availability to  
622 Symbiodinium, and Thermal Bleaching. *Front Mar Sci* 5.  
623 <https://doi.org/10.3389/fmars.2018.00450>

624 Tamir, R., Eyal, G., Cohen, I., Loya, Y., 2020. Effects of Light Pollution on the Early Life  
625 Stages of the Most Abundant Northern Red Sea Coral. *Microorganisms* 8, 193.  
626 <https://doi.org/10.3390/microorganisms8020193>

627 Tamir, R., Lerner, A., Haspel, C., Dubinsky, Z., Iluz, D., 2017. The spectral and spatial  
628 distribution of light pollution in the waters of the northern Gulf of Aqaba (Eilat). *Sci*  
629 *Rep* 7. <https://doi.org/10.1038/srep42329>

630 Team, R.C., 2023. R: A Language and Environment for Statistical Computing. R Foundation  
631 for Statistical Computing, Vienna, Austria. URL <https://www.R-project.org/>.

632 Tidau, S., Smyth, T., McKee, D., Wiedenmann, J., D'Angelo, C., Wilcockson, D., Ellison,  
633 A., Grimmer, A.J., Jenkins, S.R., Widdicombe, S., Queirós, A.M., Talbot, E., Wright,  
634 A., Davies, T.W., 2021. Marine artificial light at night: An empirical and technical  
635 guide. *Methods Ecol Evol* 12, 1588–1601. <https://doi.org/https://doi.org/10.1111/2041-210X.13653>

637 Vásquez-Elizondo, R.M., Legaria-Moreno, L., Pérez-Castro, M.Á., Krämer, W.E., Scheufen,  
638 T., Iglesias-Prieto, R., Enríquez, S., 2017. Absorptance determinations on multicellular  
639 tissues. *Photosynth Res* 132, 311–324. <https://doi.org/10.1007/s11120-017-0395-6>

640 Wang, X.Y., Xu, X.M., Cui, J., 2015. The importance of blue light for leaf area expansion,  
641 development of photosynthetic apparatus, and chloroplast ultrastructure of *Cucumis*  
642 *sativus* grown under weak light. *Photosynthetica* 53, 213–222.  
643 <https://doi.org/10.1007/s11099-015-0083-8>

644 Wangpraseurt, D., Holm, J.B., Larkum, A.W.D., Pernice, M., Ralph, P.J., Suggett, D.J., Kühl,  
645 M., 2017. In vivo microscale measurements of light and photosynthesis during coral  
646 bleaching: Evidence for the optical feedback loop? *Front Microbiol* 8, 1–12.  
647 <https://doi.org/10.3389/fmicb.2017.00059>

648 Wangpraseurt, D., Larkum, A.W.D., Ralph, P.J., Kühl, M., 2012. Light gradients and optical  
649 microniches in coral tissues. *Front Microbiol* 3, 1–9.  
650 <https://doi.org/10.3389/fmicb.2012.00316>

651 Wangpraseurt, D., Polerecky, L., Larkum, A.W.D., Ralph, P.J., Nielsen, D.A., Pernice, M.,  
652 Kühl, M., 2014. The in situ light microenvironment of corals. *Limnol Oceanogr* 59,  
653 917–926. <https://doi.org/10.4319/lo.2014.59.3.0917>

654 Zheng, L., Van Labeke, M.-C., 2017. Long-Term Effects of Red- and Blue-Light Emitting  
655 Diodes on Leaf Anatomy and Photosynthetic Efficiency of Three Ornamental Pot Plants.  
656 *Front Plant Sci* 8. <https://doi.org/10.3389/fpls.2017.00917>

657 Zissis, G., Bertoldi, P., 2018. Status of LED-lighting world market in 2017. Ispra, Italy:  
658 European Commission.

659

660

661

662

663

664

665

666

667

668

669

670

671

672

673

674

675

676

677

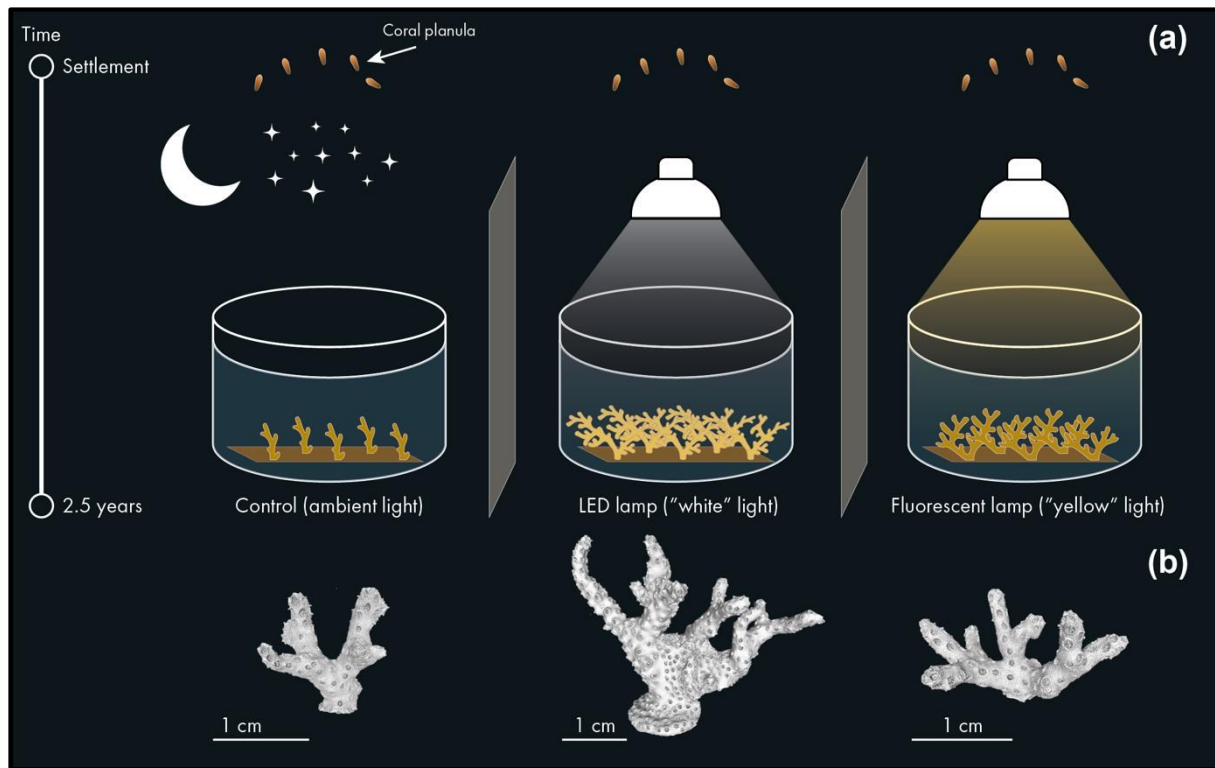
678

679

680

681

682



683

684 **Figure 1.** Schematic illustration of the experimental design. **(a)** *Stylophora pistillata* coral  
 685 planulae were collected from the shallow reef and allowed to settle and grow for 2.5 years in  
 686 three separate seawater tables. One table was kept under natural conditions, while the other two  
 687 were subjected to artificial light at night (LED and fluorescent), replicating common city  
 688 lighting methods. **(b)** 3D colonies rendered from  $\mu$ CT X-ray scans.

689

690

691

692

693

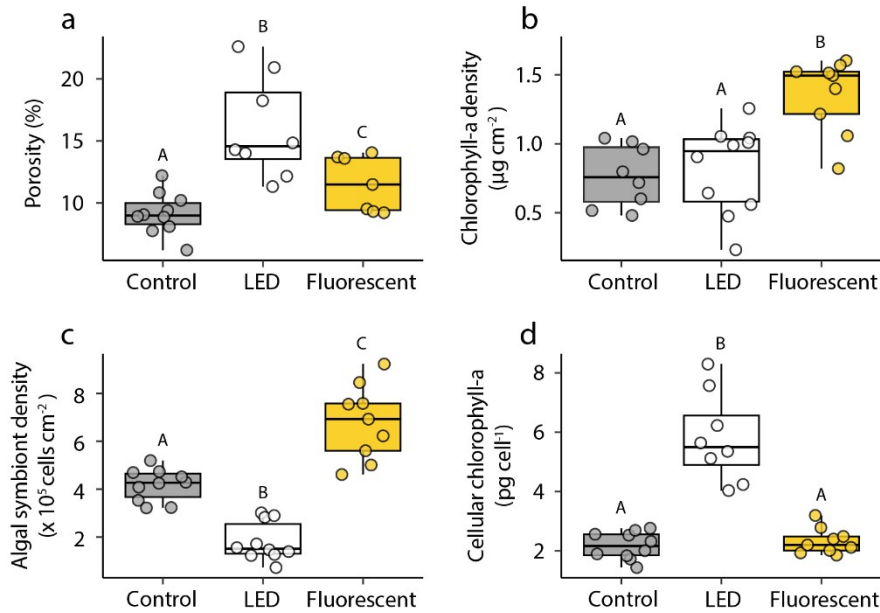
694

695

696

697

698



699

700 **Figure 2.** Boxplots showing (a) skeletal porosity, (b) Chlorophyll-a density, (c) algal symbiont  
 701 density, and (d) cellular chlorophyll-a of the experimental corals 30 months post-settlement in  
 702 the three light treatments – control (ambient; gray), fluorescent lamp (yellow), and LED lamp  
 703 (white). Horizontal lines depict the median, box height depicts the interquartile range, whiskers  
 704 depict  $\pm 1.5 \times$  interquartile range. Capital letters indicate significance among treatments.

705

706

707

708

709

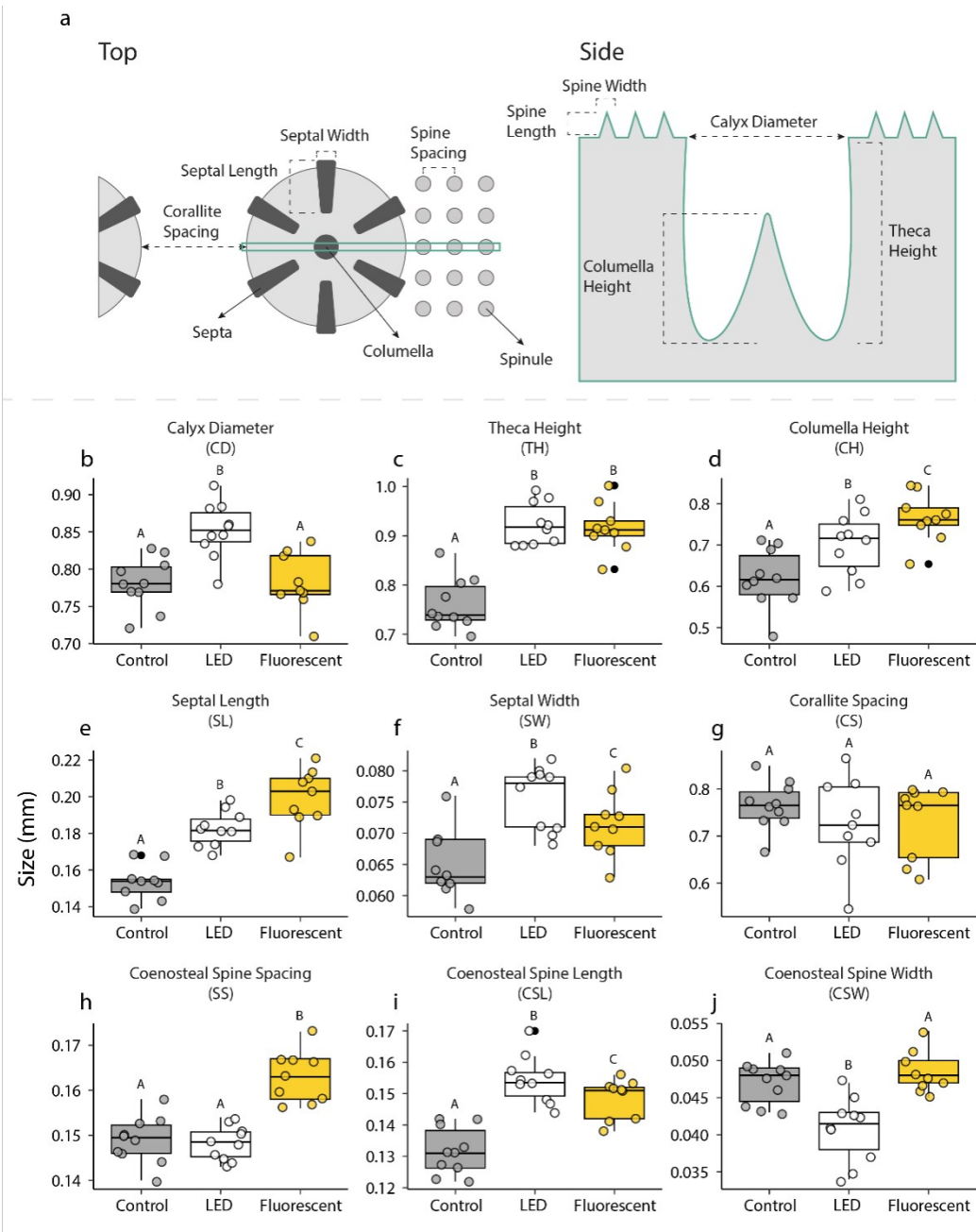
710

711

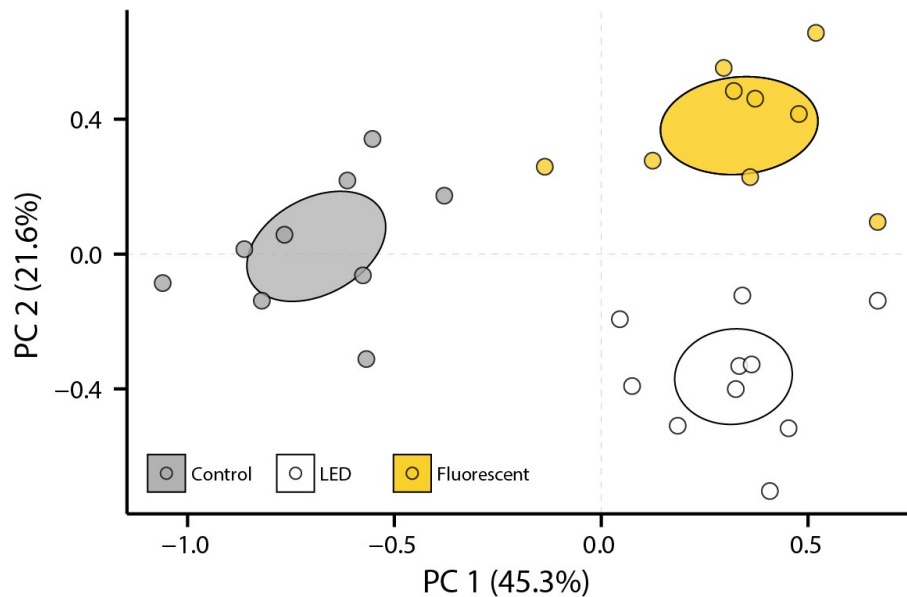
712

713

714



717 **Figure 3. (a)** A 2D illustration of the top and side views of a corallite, along with its  
718 surrounding coenosteum (modified after Kramer et al. (2022b)). **(b-j)** Morphometric results of  
719 the experimental corals' skeletal traits 30 months post-settlement for the three light treatments  
720 – control (ambient; gray), fluorescent lamp (yellow), and LED lamp (white). Horizontal lines  
721 depict the median, box height depicts the interquartile range, whiskers depict  $\pm 1.5 \times$   
722 interquartile range, and black dots represent outliers. Capital letters indicate significance  
723 among treatments.



724

725 **Figure 4.** Principal coordinate analysis (PCoA) of the morphological traits of juvenile *S.*  
 726 *pistillata* corals based on Euclidean space. Each circle represents a particular colony and is  
 727 colored by light treatment. Ellipses are standard error.

728

729

730

731

732

733

734

735

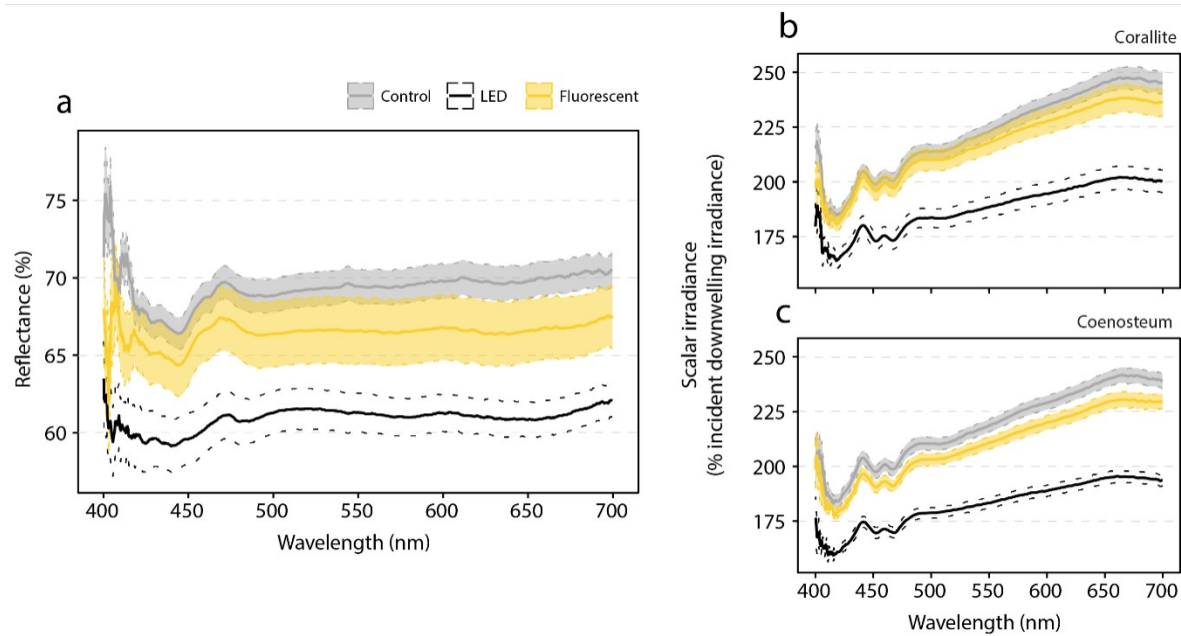
736

737

738

739

740



741

742 **Figure 5.** Apparent optical properties at 400–700 nm. **(a)** Normalized spectral reflectance of  
 743 light over the coral skeleton (%). **(b-c)** Scalar photon irradiance (% incident downwelling  
 744 irradiance) at the skeleton surface of the **(b)** corallites and **(c)** the coenosteum. Solid lines are  
 745 means, and dashed lines are standard errors.